

UV-Photo Graft Functionalization of Polyethersulfone Membrane with Strong Polyelectrolyte Hydrogel and Its Application for Nanofiltration

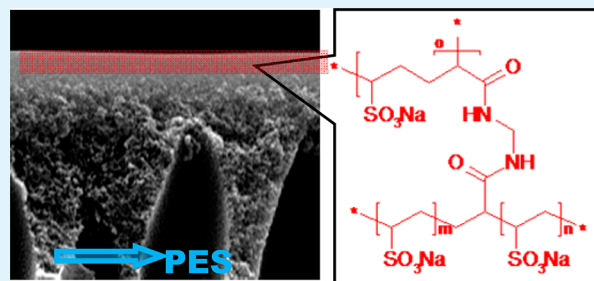
Roy Bernstein,[†] Enrique Antón,^{†,‡} and Mathias Ulbricht*,[†]

[†]Lehrstuhl für Technische Chemie II, Universität Duisburg-Essen, 45117 Essen, Germany

[‡]Department of Chemical and Environmental Engineering, University of Oviedo, 33006 Oviedo, Spain

ABSTRACT: A strong polyelectrolyte hydrogel was graft copolymerized on a polyethersulfone (PES) ultrafiltration (UF) membrane using vinyl sulfonic acid (VSA) as the functional monomer, and N,N'-methylenbisacrylamide (MBAA) as the cross-linker monomer. This was carried out in one simple step using the UV photoirradiation method. The effect of the polymerization conditions on the degree of grafting (DG) was investigated using the gravimetric method which measures the total hydrogel grafted on the membrane, and with ATR-FTIR spectroscopy which indicates the functional monomer fraction in the hydrogel layer. The VSA could not graft polymerize without the cross-linker as comonomer. An increase in the cross-linker fraction from 0.25 to 2.5 mol % (relative to the functional monomer VSA) resulted in a higher DG. Although the surface morphology changed upon modification, the resulting surface roughness as measured by AFM was very low. From the monitoring of DG with UV time (4.5–30 min) at constant conditions, it was deduced that during the early stages of the polymerization mainly the cross-linker was grafted, thus inducing the graft copolymerization of the functional monomer. Polymerization using a higher monomer concentration (12.5–40% VSA) at constant monomer/cross-linker ratio resulted in a higher VSA fraction in the grafted hydrogel, although the gravimetric DG was similar. Ion exchange capacity and X-ray photoelectron spectroscopy measured after modification under the different conditions supported these findings. The new membranes were tested under nanofiltration (NF) conditions. A NF membrane could be obtained when the MBAA fraction was above 0.25%. The Na_2SO_4 rejection was 90–99% and the permeability $10\text{--}1 \text{ L m}^{-2} \text{ h}^{-1} \text{ bar}^{-1}$ when the MBAA fraction increased from 0.75 to 2.5%. The order of rejection of single salts solution was $\text{Na}_2\text{SO}_4 > \text{MgSO}_4 \approx \text{NaCl} > \text{CaCl}_2$, as expected on the basis of Donnan exclusion for negatively charged NF membranes. An increase in the salts rejection with increasing degree of cross-linking and VSA fraction was attributed to an increase in the membrane charge density and to steric exclusion that also resulted in an increase of rejection for uncharged solutes such as sucrose or glucose. The new membrane presented a high, essentially unchanged Na_2SO_4 rejection (>97%) in the range of salt concentrations up to 4 g/L, and only slightly reduced rejection (>92%) at a concentration of 8 g/L; this can be related to its high barrier layer charge density measured by ion exchange capacity. In addition, because poly(vinyl sulfonic acid) (PVSA) is a strong polyelectrolyte the membrane separation performance was stable in the range of pH 1.5 to pH 10.

KEYWORDS: nanofiltration membrane, polyelectrolyte hydrogel, photografting, membrane modification, surface modification, vinyl sulfonic acid



INTRODUCTION

The feasibility of charged nanofiltration (NF) membranes fabrication using polyelectrolytes as the active layer is being explored in the past few years.¹ This is primarily done through two methods. The first one is synthesis of a polyelectrolyte, either inside the pores of an ultrafiltration (UF) base membrane, thus obtaining a pore-filling composite membrane,² or on the outer surface of an UF membrane, resulting in a thin-film composite membrane.^{3–5} The second method is through the deposition of polyelectrolyte, the “layer by layer” (LBL) technique, on or within a porous polymeric support,^{6,7} or inorganic support.⁸ Both techniques have already demonstrated that a NF membrane for ions separation as well as for other

applications including, for instance, forward osmosis,^{9–11} can successfully be produced using various polyelectrolytes. Yet, these membranes still have some drawbacks compared with the commercially available NF membranes that withhold their further expansion.

One of the key factors in the evaluation of the performance in membrane technology is the trade-off between the membrane selectivity and permeability. For polyelectrolyte NF membranes, the rejection of charged solutes is governed

Received: March 9, 2012

Accepted: June 18, 2012

Published: June 18, 2012



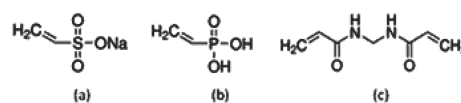
mainly by the Donnan exclusion,¹² which is a consequence of the fixed charge density of the membrane active layer. The steric exclusion, which is directly proportional to the ratio between the size of a solute and the membrane pore size¹³ and to the ratio between the active layer thickness and porosity,¹⁴ is responsible for the rejection of uncharged solutes and also contributes to the rejection of charged solutes.¹⁵ To obtain a polyelectrolyte NF membrane with high separation ability, a dense and a “defect free” high charge density polyelectrolyte active layer must be obtained. Therefore, the number of the polyelectrolyte layers deposited on the porous membrane, or the degree of functionalization, should usually be high. However, since membrane permeability is controlled by the active layer pore size distribution, thickness and swelling,^{16,17} the consequence is a membrane with reduced permeability. The trade-off between rejection and permeability of polyelectrolyte membranes can be optimized by changing the fabrication conditions and the active layer composition.^{2,8} Nevertheless, the performance of the majority of the previously presented NF membranes fabricated by the polymerization method was not better than the commercial ones. On the other hand, the “LBL” method, which can produce a membrane having high performance, is time-consuming, requires several steps, and still presents a challenge to scale-up for commercial application.^{9,18}

A different approach to the fabrication of charged NF membrane may be graft copolymerization of a polyelectrolyte hydrogel on a UF support.¹⁹ A hydrogel is a cross-linked polymer network (via chemical or physical interaction), swollen with water, yet insoluble because of the high cross-linking degree. For in situ polymerized hydrogels, swelling, which influences membrane permeability, is mainly controlled by the ratio between the cross-linker monomer and the functional monomer.¹⁹ Therefore, the reduced permeability following surface modification using hydrogel as the active layer might be adjusted. Hydrogels are also well recognized for their relatively small mesh size, which can assist in promoting the membrane selectivity by sieving.²⁰ In addition, using a charged monomer for the hydrogel synthesis, a highly charged active layer, and thus a high Donnan exclusion may be attained.²¹

The photoirradiation-induced radical graft copolymerization technique was recently successfully applied for surface modification of hydrogels on UF membranes.^{22,23} This technique has several advantages: it generates a rapid reaction and is performed under mild conditions with various monomers using simple equipment at a relatively low cost. The polymerization using this technique is mostly surface specific—it is limited to a narrow region close to the outer membrane surface. This technique can also be implemented for commercial production.²⁴ Moreover, when the modification is performed using a UV-active UF membrane, i.e., the membrane polymer undergoes a homolytic chain cleavage resulting in free radicals on its surface (such as polyethersulfone, PES), the polymerization does not require photoinitiator agents.²⁴

In this research, the possibility to graft polymerize a strong polyelectrolyte hydrogel on a commercial PES UF membrane through the photoinitiation technique was investigated. Two charged monomers, vinyl phosphonic acid and vinyl sulfonic acid, with N,N'-methylenebisacrylamide as a cross-linker monomer, were evaluated for the polymerization of the polyelectrolyte hydrogel (Scheme 1). These monomers were selected on the assumption that a swollen, high charge density polyelectrolyte hydrogel, which will also be ionizable

Scheme 1. Chemical Structure of the Functional Monomers and Cross-Linker Monomer Used in This Research: (a) VSA, (b) VPA, and (c) MBAA



throughout the entire pH range, will be obtained. In addition, the content of cross-linker monomer was varied in order to identify its effects onto charge density and sieving. To the best of our knowledge, these monomers were not used previously for fabrication of a NF membrane using the radical graft copolymerization technique. Therefore, this research investigated the feasibility of using these monomers for fabrication of a polyelectrolyte hydrogel membrane and the effect of the polymerization conditions on the modification efficiency as well as on the membrane characteristics. Then, the new membranes were tested for their performance under NF conditions, also at various pH values and at different salinities.

EXPERIMENTAL SECTION

Materials. The PES membranes were supplied by Sartorius AG (Germany) with nominal molecular weight cut off (MWCO) of 30 kDa as reported by the manufacturer. It should be noted, however, that it was recently found that for these membranes the reported MWCO is different from the MWCO measured with dextran mixtures and that the 30 kDa membrane has a measured MWCO of approximately 90 kDa.²⁵ Prior to the modification, the membranes were cut with a 56 mm diameter punch hole and washed in methanol for 1 h, then thoroughly washed with Milli-Q water and left in Milli-Q water until used. Vinylsulfonic acid sodium salt (VSA; 25%) from Sigma-Aldrich and vinyl phosphonic acid (VPA) from BASF were used as monomers, and N,N'-methylenebisacrylamide (MBAA) from Sigma-Aldrich was used as the cross-linker (Scheme 1). The monomers and cross-linkers were used as received. To obtain monomer solution with 40% VSA, we concentrated the 25% VSA solution under reduced pressure at 37 mbar and 45 °C. The monomer concentration was 40% when the solution density was 1.32 g/L. MgSO₄, NaCl, Na₂SO₄, and CaCl₂ and glucose were purchased from Sigma-Aldrich. Sucrose was purchased from Acros, Geel, Belgium. These test substances were used without purification. All experiments were done with purified water from a Milli-Q system from Millipore.

Modification Procedure. A water-wet membrane was placed in a glass holder, leaving only the outer surface of the membrane (diameter 54 mm) in contact with the solution, and remained covered with Milli-Q water until modification. The water was then wiped off with a tissue paper and the membrane surface was covered with 5 mL modification solution (previously degassed with nitrogen for 10 min). Thereafter, the sample was placed inside a UV system (UVA Cube 2000, Höne AG, Germany, equipped with a 20 cm long mercury lamp, allowing a homogeneous irradiation of 0.1 m² area via reflecting walls). The membrane was thereafter irradiated at 55 ± 5 mW/cm², unless stated otherwise, for different times (2–35 min). The UV wavelength was narrowed to $\lambda = 315$ –400 nm, by using a special filter glass in order to avoid membrane degradation.²⁶ At the end of the modification, the membrane was washed with Milli-Q water for 24 h at room temperature. To verify chemical grafting, we washed a few membranes at 50 °C for 48 h with Milli-Q water or with ethanol. Negligible differences in performance were found for membranes which were washed at the different conditions. The modification was performed with VSA or VPA as the functional monomers and MBAA as the cross-linker monomer. No modification occurred when VPA was used as a monomer under all conditions tested. Therefore, only results with VSA are presented.

Degree of Grafting. The degree of grafting (DG) was calculated using the gravimetry (DG_g) and spectrometry (DG_s) methods.

DG_s was determined by attenuated total reflection Fourier transform infrared (FTIR-ATR) spectroscopy (Varian 3100, USA equipped with a one reflection KRS-5 crystal, 45°, 64 scans were taken for each spectrum at a resolution of 4 cm^{-1}) and defined as follows:

$$DG_s = \frac{I_{\text{mon}}}{I_{\text{mem}}} \quad (1)$$

where I_{mon} is the intensity of the 1040 cm^{-1} band assigned to the symmetric stretching of the VSA sulfonate group and I_{mem} is the intensity of the 1577 cm^{-1} band, a C–H peak from the aromatic ring in the base PES membrane which does not appear in the monomer or the cross-linker IR spectra. The reported values are the average values of at least 5 distinct samples for every condition and every sample was measured at three different locations and the errors being standard deviations.

For the determination of DG_g , unmodified and modified membranes were cut with the same punch-hole (either 7 or 25 mm), dried for 24 h at 40 °C in a vacuum, and left in a desiccator for few hours before weighing. The DG_g was obtained using

$$DG_g = \frac{m_{\text{modified}} - m_{\text{PES}}}{A} \quad (2)$$

where m_{modified} is the weight of a modified membrane, m_{PES} is the average weight of at least three unmodified PES membranes, and A is the membrane area. DG_g was calculated under the assumption that samples from a specific unmodified membrane cut with a punch-hole at the same diameter have the same weight. This was found very accurate; for example, the weight of 7 different samples from pristine PES membranes was (7.036 ± 0.050) mg (i.e., less than 7% variation). The reported values are the average of at least 3 distinct membranes when at least two samples were cut from each membrane. Samples from the same membrane with more than 10% difference were excluded.

The gravimetric method was used since it was found that drying the membrane before modification results in a change of its properties. Additionally, the DG_s is directly correlated with the newly introduced polymer concentration on the surface, whereas, the DG_g is an indication of the total mass of the modification layer. Hence, the cross-linker content in the modification layer may be estimated from the difference in the DG measured using the two methods.

Membrane Characterization. Ion Exchange Capacity (IEC). Modified and pristine membranes that were cut with a punch-hole (25 mm diameter), were submerged in 1 M HCl solution for 24 h. The solution was replaced once during this time in order to ensure complete conversion of the sulfonic group to its acid form. After 24 h, the membranes were washed with Milli-Q water and immersed for 24 h in 10 mL 2 M NaCl solution to convert the sulfonic acid group to its Na^+ form. The solution was replaced 5 times, so that a total solution of 50 mL was collected. The solution was then titrated with 0.01 N NaOH using a Mettler Toledo (T90) titrator. The membranes were then washed thoroughly with Milli-Q water, dried for 24 h in a vacuum oven at 40 °C and weighed. The IEC [mequiv g^{-1}] was calculated using:

$$\text{IEC} = \frac{(V - V_0)c}{w} \quad (3)$$

where V is the volume of NaOH [mL] needed for the back-titration, V_0 is the average volume for the titration of three PES control samples, c is the NaOH concentration [M] and w is weight of the modification layer [g], measured as the difference between the weight of the modified and the unmodified control PES membrane.

X-ray Photoelectron Spectroscopy (XPS). XPS general survey spectra and high-resolution spectra were recorded using ESCALAB 250 (Thermo Fisher Scientific Inc., Waltham, UK) with Al X-ray source and monochromator. Binding energies for probed elements were corrected for the charging effect with reference to the 285 eV C1s peak.

Atomic Force Microscopy. (AFM) images of a dry pristine and a dry modified membrane were obtained using a MultiMode AFM with

Nanoscope IIIa controller and equipped with a 10 μm scanner from Digital Instruments, Santa Barbara, CA, USA. The measurements were performed in a tapping mode with a silicon tip having a radius of <10 nm. Average root-mean-square roughness (rms) of 3 distinct samples was obtained at surface areas of 2 $\mu\text{m} \times 2 \mu\text{m}$.

Membrane Performance. The membranes were cut with a punch hole (44 mm) and placed in a dead end cell (Amicon 8050) connected to a reservoir. Salt rejection and permeability were measured at 2–4 bar (pressurized with nitrogen) at 600–700 rpm stirring rate. Salt rejection was calculated by

$$\text{rejection} = 1 - \frac{C_p}{C_f} \quad (4)$$

where C_f and C_p are the salt concentration in the feed and permeate, respectively. Salt concentration was measured using conductometry. Membrane permeability (L_p) using Milli-Q water was determined by

$$L_p = \frac{V}{AtP} \quad (5)$$

where V is the water volume collected (L), A is the membrane area (m^2), t time (h), and P is the applied pressure (bar).

Sucrose and glucose rejection, separately, were measured at the same conditions as the salt rejection experiment, and at a concentration of 1 mM. The solute concentrations in the feed and in the permeate were measured by TOC analyzer (Shimadzu, Japan, Model: TOC-VCSH).

The effect of salt concentration on rejection was determined at four Na_2SO_4 concentrations (1–8 g/L). The experiments were conducted at the same trans-membrane pressure (TMP) of 3.1 bar, except for the experiment at 8 g/L which was done at TMP of 1.5 bar. This was because the maximum operating pressures allowed using the Amicon 8050 cell is ~ 5 bar, and the osmotic pressure of 8 g/L Na_2SO_4 is approximately 3.5 bar.

Membrane stability and performance were tested at three pH values (1.5–2, 7 and 10) by soaking six analogous modified membranes (25% VSA, 1.5% MBAA, $t = 18$ min, $I = 55 \text{ mW/cm}^2$) in solutions of low and higher pH, three in Milli-Q water at pH 2 and three in Milli-Q water at pH 10. Every 24 h, one membrane was removed from the solution and its performance was measured once (the last membrane was measured after 6 days). Every membrane was tested at the three pH values as follows: first the flux and rejection were measured at the pH that it was soaked in (the membrane that was soaked at pH 2 was measured at pH 1.5), then it was washed with Milli-Q water and thereafter it was tested with salt solutions at the other two pH values. The membranes were tested with 1 g/L Na_2SO_4 and at a pressure of 4 bar. The pH was adjusted using H_2SO_4 or NaOH.

RESULTS AND DISCUSSION

Degree of Functionalization As Function of Modification Conditions. Figure 1 presents the IR spectra, measured using ATR-FTIR, of the pristine and the modified membranes with 25 wt % VSA as monomer and with different cross-linker concentrations (mole%, relative to VSA).

A new band assigned to the stretching vibration of the sulfonic acid group of the monomer is seen at 1040 cm^{-1} . The intensity of this band increases with cross-linker concentration indicating an increase in the modification degree. The other band marked at 1577 cm^{-1} is of the base membrane and is used for the DGs calculations (eq 1). Two bands attributed to the cross-linker are observed at 1543 cm^{-1} and at 1662 cm^{-1} and are ascribed to the amide I ($\text{C}=\text{O}$) and the amide II ($\text{N}-\text{H}$) absorption, respectively. The former appears only at high cross-linker concentration. The latter also appears in the pristine PES membrane spectrum, although at a much lower intensity, and it also shifts to 1680 cm^{-1} . This is probably as a result of poly-N-vinylpyrrolidone (PVP) added to the PES by the manufacturer.²⁷ Another new band resulting from the modification is

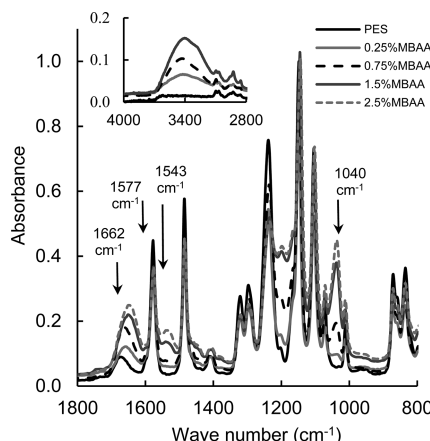


Figure 1. ATR-FTIR of the pristine and modified membranes prepared with different cross-linker concentration. Modification conditions: 25% VSA, $t = 18$ min, $I = 55$ mW/cm 2 .

seen in Figure 1 in the range 3000–3400 cm $^{-1}$ and is attributed to hydrogen bonds.²⁸

Figure 2 shows the degree of modification obtained at different cross-linker concentrations under otherwise constant modification conditions.

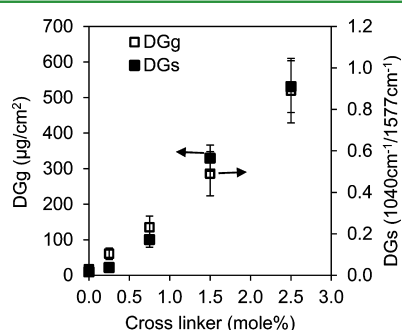


Figure 2. Degree of grafting measured using the spectroscopic (DG_s) and gravimetric (DG_g) methods after modification at different cross-linker fractions (mole %). Modification conditions: 25% VSA, $t = 18$ min, $I = 55$ mW/cm 2 , $n \geq 5$.

The degrees of modification measured by the two techniques have a similar trend: a linear increase in the DG with cross-linker concentration. The DG without cross-linker was very low. This is probably a consequence of wetting or diffusion limitation due to incompatibility between the charged monomer and the hydrophobic surface.^{29,30} Figure 2 demonstrates that by adding the cross-linker as a comonomer at a low concentration, the VSA can easily be graft copolymerized on a PES membrane. This contrasts a previous report which argued that radical co-polymerization of VSA with MBAA (using ammonium peroxydisulfate as initiator) to form a hydrogel cannot occur.³¹ Furthermore, although the copolymerization of VSA and MBAA is similar to copolymerization of VSA with other hydrophilic monomers, due to the low concentration of the MBAA, a hydrogel with high PVSA content can be obtained. In contrast, the VSA fraction when copolymerized with acrylic acid (AA) could only be as high as 25 wt %, and copolymerization of VSA with AA and divinyl benzene resulted only in a 5% PVSA fraction in the gel, regardless of the VSA content used during the polymerization.^{31,32}

It was interesting to find out that despite the similar structure of VSA and VPA (Scheme 1) a hydrogel using VPA as a monomer could not be obtained. The reason was not investigated in this research, but it is known that polymerization of VPA by radical polymerization is very difficult and occurs only at high temperature.^{33,34} This may be related to the fact that the charge density of VPA is even higher than that of VSA, and that chain propagation is hindered by electrostatic repulsion. Moreover, no report of surface grafting of VPA using radical polymerization was found in the literature.

Figure 3 describes the modification progress with modification time with 1.5 and 2.5% cross-linker fraction under

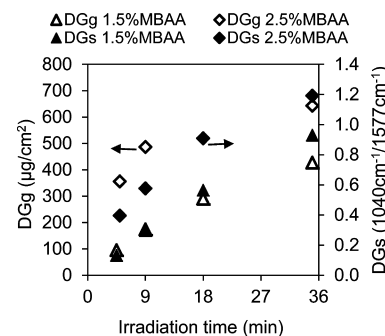


Figure 3. Modification progress presented as the DG_s (solid markers) and DG_g (empty markers) at two cross-linker fractions (1.5 and 2.5% MBAA). Modification conditions: 25% VSA, $I = 55$ mW/cm 2 , $n \geq 3$.

otherwise constant conditions. The increase of the DG_s with modification time is monotonic. However, the DG_g rises fast in the early stages and then the increase moderates. Moreover, the rise and the moderation occur faster with the higher cross-linker concentration. Therefore, it can be assumed that in the early stages it is mainly the cross-linker monomer that is grafted to the surface, and then, either because of the cross-linker's two double bonds or a change in the surface properties, the functional monomer (VSA) grafting is enhanced. This facilitating role of MBAA was also recognized by Wu et al.³⁵ using the functional monomer N-vinyl-2-pyrrolidone, which can be graft copolymerized without a cross-linker at higher degree than VSA.

The effect of the monomer concentration was also investigated by comparing the ratio of the modification degree measured using the two techniques (Figure 4). The data labels in Figure 4 indicate the cross-linker concentration (mole%). The cross-linker concentration when the modification was carried out without the functional monomer (0% VSA) was the same as for modification with 25% VSA.

The ratio between the DG_s and the DG_g using the 12.5% VSA solutions is much lower than with 25 and 40% VSA, although the modification time was higher (18 and 35 min for 12.5 and 25 and 40% VSA, respectively). This can be explained by a higher cross-linker fraction in the modification layer when using 12.5% VSA in comparison with modification at 25% VSA. The ratio between DG_g and DG_s for 25% VSA and 40% VSA is similar (Figure 4). However, to achieve a similar modification degree, the required cross-linker concentration using 40% VSA is lower.

The effect of the irradiation intensity on the modification, using similar energy doses, is described in Figure 5. Considering the low modification degree with only VSA, the experiments were conducted mainly at a high intensity (55 mW/cm 2) and

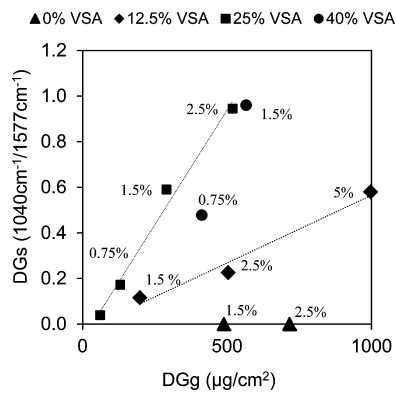


Figure 4. DG_s vs DG_g following modification obtained with different monomer concentration (0, 12.5, 25, and 40% VSA), different cross-linker fraction (0.25–5% MBAA), and different modification times (18 and 35 min); modification conditions: $I = 55 \text{ mW/cm}^2$, $n \geq 3$.

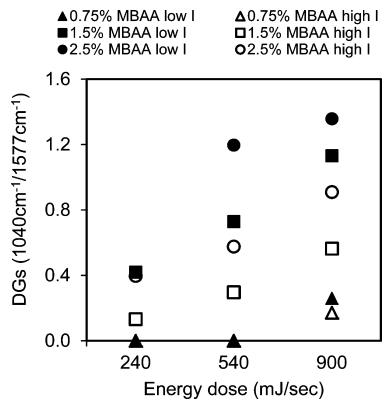


Figure 5. Effect of high ($I = 55 \text{ mW/cm}^2$, empty marker) and low ($I = 16 \text{ mW/cm}^2$, solid marker) irradiation intensities on spectroscopy degree of grafting at different cross-linker concentrations (0.75–2.5% MBAA) and energy doses, $n \geq 3$.

with high energy doses. Nevertheless, Figure 5 clearly shows that irradiation at low intensity (16 mW/cm^2) results in high modification compared with irradiation at high intensity. Generally, it is accepted that the polymerization rate can increase with irradiation intensity.^{36,37} However, polymerization at too high intensities can be monomer diffusion limited immediately in the early stages, due to the high initiator radicals concentration, whereas for polymerization at low UV intensities, the diffusion limitation occurs at later stage.³⁸ This can change the monomer conversion,³⁹ and hence, the modification degree as well as the modification layer structure and properties.⁴⁰ It was also demonstrated, for membrane modification using redox radical polymerization, that when a too high initial radical concentration was used, lower modification degrees were measured, probably because of enhanced efficiency of the termination reaction over the propagation reaction.⁴¹ Additionally, high intensity may result in membrane degradation,²³ which might also influence the modification degree.

Surface Characterization. The IEC of membranes modified at different conditions is shown in Table 1. Modification without a cross-linker resulted in an IEC similar to the theoretical value of PVSA (9 mequiv g^{-1}), but it was difficult to determine exactly because of the low degree of modification.

Table 1. Ion Exchange Capacity of Modified Membranes with Similar DG_g Prepared at Different Cross-Linker Fractions, Different Modification Time, and Different Monomer Concentration^a

VSA (%)	MBAA (mole %)	modification time (min)	IEC (mequiv g^{-1})
25	0.25	18	3.2 ± 0.2
25	0.75	18	2.8 ± 0.3
25	1.5	18	3.1 ± 0.4
25	2.5	18	3.1 ± 0.1
25	1.5	4.5	1.4 ± 0.4
25	1.5	9	2.2 ± 0.2
25	1.5	35	3.3 ± 0.2
12.5	2.5	35	1.9 ± 0.4
40	1.5	18	4.3 ± 0.7

^aModification conditions: $I = 55 \text{ mW/cm}^2$, $n \geq 3$.

The IEC for membranes prepared with a cross-linker was lower than the theoretical value for PVSA at all conditions, indicating a relatively high cross-linker fraction in the active layer, as was also reported previously for other functional monomers.⁴⁰ Still, these IEC values are rather high compared to other charged NF membranes,^{40,42} prompting a high Donnan exclusion. Surprisingly, the IEC values at 25% VSA were similar at the different cross-linker concentrations. Thus, it may be speculated that the cross-linker fraction is not very different in the modification layer obtained after varied conditions. On the other hand, increasing the VSA concentration to 40% (at same MBAA concentration, 1.5%, and UV time, 8 min; cf. Table 1) resulted in a higher IEC, i.e., higher VSA fraction in the modified layer. This can be explained by the effect of monomer ratio onto chain propagation and also illustrates that by altering some of the polymerization conditions the VSA fraction in the copolymer hydrogel can be increased.

The IEC at the various modification times and at a constant MBAA concentration (1.5%) is also presented in Table 1. The IEC in the early stages is low and it increases with the modification progress, until it levels off (at 18 min). This reflects the increase in the VSA content during the modification progress, as discussed before (cf. Figure 3).

The increased cross-linker fraction in the modification layer at lower monomer concentration and at the early stages of the modification was also established using elemental analysis of the modified layer at the three monomer concentrations and the different modification times as presented in Table 2.

The pristine PES membrane contains nitrogen, probably because of modification with the additive PVP.²⁷ The C:O ratio of the modified membranes is much higher than the theoretical value for the VSA. This confirms that the modification layer has relatively high cross-linker fraction because this ratio is much higher for MBAA than for VSA. High resolution XPS revealed the disappearance of the C1s band at 291.1 eV associated with aromatic $\pi-\pi^*$ carbon and was recorded at 3% only on the unmodified PES membrane, demonstrating complete coverage of the surface of the PES base membrane. The N:S and C:O ratios decrease with modification time and with monomer concentrations for membranes having similar DG_g . This concurs with the previous assumption that the modification layer has a higher cross-linker fraction at these conditions because the functional monomer VSA does not contain nitrogen.

Table 2. Elemental Composition (in atomic percent) and Ratios Obtained by XPS for Pristine and Modified PES Membranes^a

	%C (285.0 eV)	%O (531.7 eV)	%S (168.0 eV)	%N (399.8 eV)	N/S	C/O	DG _s	DG _g ($\mu\text{g}/\text{cm}^2$)
PES theoretical	75.0	18.8	6.2			3.99		
PES pristine	72.2	18.0	4.7	4.9	1.04	4.30		
VSA theoretical	33.3	50.0	16.7			0.67		
MBAA theoretical	64.0	18.0			18.0	3.56		
25% VSA, 1.5% MBAA, $t = 9$ min.	71.6	18.7	4.0	5.6	1.40	3.83		
12.5% VSA, 2.5% MBAA, $t = 18$ min	73.0	18.6	3.1	5.4	1.74	3.92	0.110	438
25% VSA, 1.5% MBAA, $t = 18$ min.	63.4	23.6	6.1	7.0	1.14	2.69	0.636	337
40% VSA, 1.5% MBAA, $t = 18$ min.	62.0	26.7	6.9	4.4	0.64	2.32	0.440	490

^aModification conditions: $I = 55 \text{ mW}/\text{cm}^2$.

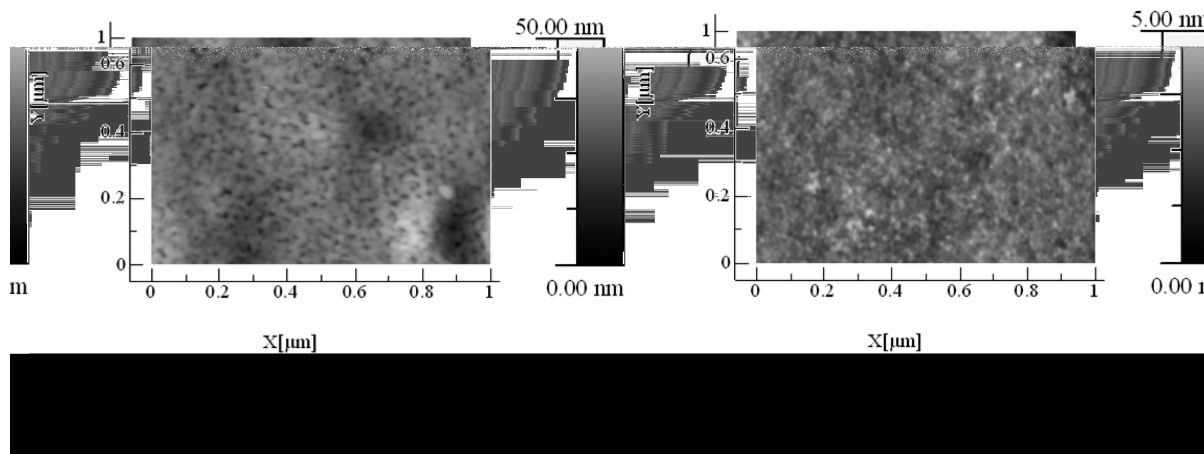


Figure 6. AFM images of unmodified PES membrane (left) and modified PES membrane (right, DG_s = 0.6). Modification conditions: 1.5% MBAA, 25% VSA, $t = 18$ min.

Surface Morphology. The change in the membrane surface morphology between the pristine PES membrane and the PES membrane after grafting at high DGs (0.6) is evident in the AFM images in Figure 6. Because the UV light can penetrate into the PES membrane, some modification takes also place within the membrane pores.²² Recently, the modification depth under analogous conditions had been analyzed by scanning electron microscopy and energy dispersive X-ray spectroscopy and found to be up to 5 μm .²⁷ Therefore, the membrane barrier layer structure can also be described as pore-filling hydrogel composite combined with a thin film hydrogel on the outer surface.

Surprisingly, although the surface morphology changed, the surface roughness which usually increases following graft copolymer modification,^{6,11,41,43} decreased from $6 \pm 3 \text{ nm}$ to $4 \pm 2 \text{ nm}$. This is lower than the roughness of most NF membranes.^{4,10,11,44} Because the membrane roughness promotes fouling phenomena in NF⁴⁵ the very low roughness might reduce the novel membranes' propensity to fouling and biofouling. The low roughness also illustrates the uniform coverage of the membrane surface by the grafted polymeric hydrogel.^{41,43}

Nanofiltration Membrane Performance. Figure 7 presents the membrane permeability and salt rejection following modification with 25% VSA at different cross-linker concentrations and of a commercial NF membrane (NF 270 Dow Filmtec).^{44,46}

A NF membrane was successfully obtained (defined herein when the Na₂SO₄ rejection was higher than 90%) when the cross-linker fraction was 0.75%. The salt rejection increased, whereas the permeability decreased with increasing cross-linker

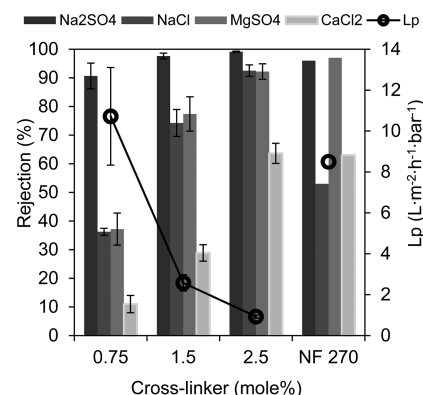


Figure 7. Salt rejection and permeability of membranes following modification at different cross-linker fractions. Modification conditions: $I = 55 \text{ mW}/\text{cm}^2$, $t = 18$ min. Filtration conditions: $P = 4 \text{ bar}$, salt concentration 1 g/L, $n \geq 3$. Commercial thin-film polyamide composite membrane for comparison.

concentration, and this was in agreement with increased DG (cf. Figure 2).

The salt rejection was in the order Na₂SO₄ > MgSO₄ ≈ NaCl > CaCl₂, as expected for rejection based on Donnan exclusion for negatively charged NF membranes.⁴⁷ The higher rejection at a higher cross-linker concentration can be attributed to steric exclusion, because the IEC was similar following modification above 0.75% MBAA (see Figure 3 and Table 1). Because rejection of uncharged solutes with charged NF membranes derives mainly from steric exclusion,⁴⁸ the increased rejection of the uncharged sucrose and glucose with increasing cross-linker

concentration (Figure 8), supports the increased steric influence by the more tightly cross-linked polyelectrolyte hydrogel.

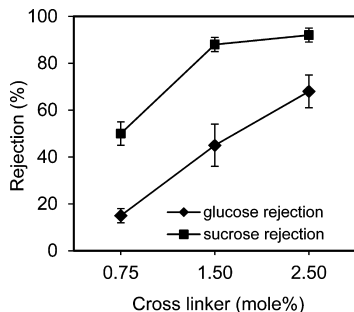


Figure 8. Sucrose and glucose rejection of membranes following modification (25% VSA, $I = 55 \text{ mW/cm}^2$, $t = 18 \text{ min}$) with different cross-linker fractions. Nanofiltration conditions: $P = 4 \text{ bar}$, 1 mM sucrose or glucose in water, $n \geq 3$.

The salt rejection of the new membrane is comparable to that of various other types of NF membranes presented before.^{2,4,6,8,46,49–52} However, the permeability is still lower than that of polyelectrolyte membranes fabricated using the “LBL” method and of a commercial polyamide-based membrane (Figure 7). Because the Donnan potential of polyelectrolyte membranes is higher than that of polyamide membranes the better performance of the latter can be attributed to the dielectric phenomena⁵³ which are probably not significant for polyelectrolyte membranes. Nevertheless, the hydrogel polyelectrolyte membranes have an optimization potential. For example, by increasing the monomer concentration, the IEC (and therefore the Donnan potential) also increased (Table 2). Moreover, such optimization was already demonstrated for polyelectrolyte membranes fabricated using the “LBL” method. These membranes presented a very low permeability when first introduced.^{54,55} The performance was then successfully optimized, almost surpassing that of the polyamide membranes.⁹ The effect of the various functionalization parameters including the influence of the base membrane pore structure and permeability on the composite membrane performance is the subject of a subsequent report.

Influence of the Salt Concentration and pH Value on NF Performance. Figure 9 describes the influence of the concentration of the Na_2SO_4 on the membrane rejection.

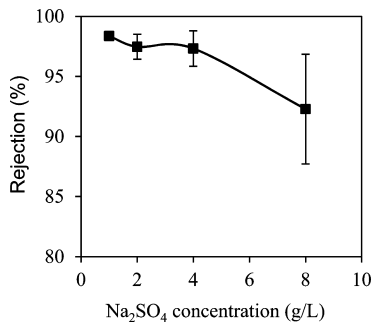


Figure 9. Na_2SO_4 rejections at various salt concentrations. Modification conditions: 25% VSA and 1.5% MBAA, $I = 55 \text{ mW/cm}^2$, and $t = 18 \text{ min}$. Filtration conditions: For 1–4 g/L, transmembrane pressure (TMP) 3.1 bar; for 8 g/L, TMP 1.5 bar.

The salt rejection was stable with increased salt concentration up to 4 g/L Na_2SO_4 (28 mM) and then decreased at 8 g/L (56 mM). The reduced rejection is probably caused by a decrease in Donnan exclusion. However, the rejection remains high due to the high IEC which suppresses the effect of the salt concentration on the membrane rejection. The lower rejection at 8 g/L is also a result of the lower permeate flux due to the lower TMP (for reasons, see Experimental Section), which can reduce the rejection significantly.⁵¹ Although it is difficult to compare the effect on the salt rejection obtained in this study to other studies because of various operation conditions and the use of different salts, it seems that the influence of salt concentrations on the rejection of new membrane is lower than for many other NF membranes fabricated by various methods.^{40,44,51,55–57}

The effects of the feed pH on the rejection of Na_2SO_4 , as well as the stability of membrane performance after being soaked in alkaline and acidic solutions are demonstrated in Figure 10.

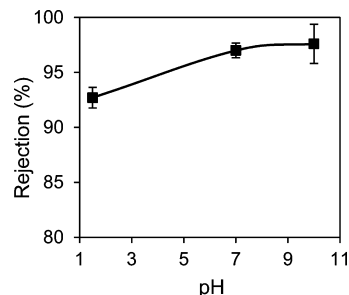


Figure 10. Rejection of Na_2SO_4 at pH 1.5, pH 7, and pH 10. Modification conditions: 25% VSA, 1.5% MBAA, $I = 55 \text{ mW/cm}^2$, and $t = 18 \text{ min}$. Filtration conditions: $P = 4 \text{ bar}$, 1 g/L Na_2SO_4 .

The rejection at pH 10 and pH 7 was similar, and it decreased slightly in acidic pH 1.5. However, it is noted that because the pH was adjusted with H_2SO_4 the SO_4^{2-} concentration at pH 1.5 was similar to the one obtained between 4–8 g/L Na_2SO_4 (as was also confirmed by conductivity measurement), thus, it can be estimated that the rejection was almost not influenced due to the low pH value. Moreover, salt rejection of membranes that were first tested in pH 1.5 and then at pH 7 was similar to the one measured for membranes that were left only in Milli-Q water (were not soaked in pH 2) before the filtration tests. The high rejection at low pH values and the stability of the membrane in acidic pH is due to the strong polyelectrolyte hydrogel. This is usually not observed for weak or uncharged NF membranes including commercial polyamide-based membranes.^{7,46,58}

CONCLUSIONS

A strong polyelectrolyte hydrogel was graft copolymerized on a PES UF membrane using vinyl sulfonic acid as the monomer and $\text{N,N}'\text{methylenbisacrylamide}$ as the cross-linker monomer. The modification was carried out in one simple step, in aqueous solution and at room temperature using the photoirradiation method. The cross-linker and the functional monomer concentration had a significant influence on the polymerization. As the cross-linker concentration increased both the DG_g and DG_s increased simultaneously. It was also demonstrated that during the early stages of the modification, mainly the cross-linker was grafted, which then facilitated the graft copoly-

merization of the functional monomer. In contrast, when the monomer concentration was low, the DG_s was substantially lower compared with the DG_g . This was explained as a result of a higher cross-linker fraction in the hydrogel. XPS and IEC supported these findings. In addition it was found that when the modification was carried out using low UV intensity the modification degree and the membrane performance were better than for modification at high UV intensity.

A NF membrane was successfully fabricated using the proposed method. The order of rejection of single salts was $\text{Na}_2\text{SO}_4 > \text{MgSO}_4 \approx \text{NaCl} > \text{CaCl}_2$, as is expected for the Donnan exclusion of negatively charged NF membranes. A further increase in the salt rejection with modification degree was attributed to an increase in the steric exclusion: The higher degree of modification also induced an increased rejection of uncharged solutes and a corresponding characteristic decrease in the membrane permeability. One advantage of conducting the polymerization using VSA as a functional monomer was evident by the very low surface roughness as measured using AFM which was lower than for most commercial or previously reported NF membranes. The strong acidity of the VSA monomer enabled the membrane to be stable while maintaining a high selectivity at low pH value. The ion exchange capacity was higher than for most charged NF membranes reported in the literature. As a consequence the new membrane had a high salt rejection (especially for sulfate), which was also maintained at relatively high salt concentrations. These features, together with the many possibilities for tailoring the membrane properties and performance, make the here reported material a promising membrane for NF as well as for other applications, for instance forward osmosis. The optimization of the polymerization conditions, the influence of the base membrane pore structure (MWCO) and their effects on membrane performance will be presented in a following paper.

AUTHOR INFORMATION

Corresponding Author

*E-mail: mathias.ulbricht@uni-essen.de.

Notes

The authors declare no competing financial interest.

ACKNOWLEDGMENTS

R.B. gratefully acknowledges the 'Young Scientists Exchange Program' of the BMBF-MOST Water Technology Cooperation for the financial support. Further thanks are due to Dr. Steffen Franzka, University Duisburg-Essen, and Yair Kaufman, Ben-Gurion University, Beer-Sheva, Israel, for performing and analyzing the AFM measurements. The XPS analyses were performed by Dr. Natalya Froumin (Ben-Gurion University).

REFERENCES

- (1) Ulbricht, M. *Polymer* **2006**, *47*, 2217–2262.
- (2) Childs, R. F.; Mika, A. M.; Pandey, A. K.; McCrory, C.; Mouton, S.; Dickson, J. M. *Sep. Purif. Technol.* **2001**, *22*, 507–517.
- (3) Du, R.; Zhao, J. *J. Membr. Sci.* **2004**, *239*, 183–188.
- (4) Deng, H.; Xu, Y.; Chen, Q.; Wei, X.; Zhu, B. *J. Membr. Sci.* **2011**, *366*, 363–372.
- (5) Qiu, C.; Nguyen, Q. T.; Ping, Z. *J. Membr. Sci.* **2007**, *295*, 88–94.
- (6) Deng, H. Y.; Xu, Y. Y.; Zhu, B. K.; Wei, X. Z.; Liu, F.; Cui, Z. Y. *J. Membr. Sci.* **2008**, *323*, 125–133.
- (7) Hollman, A. M.; Bhattacharyya, D. *Langmuir* **2004**, *20*, 5418–5424.

- (8) Miller, M. D.; Bruening, M. L. *Langmuir* **2004**, *20*, 11545–11551.
- (9) Bruening, M. L.; Dotzauer, D. M.; Jain, P.; Ouyang, L.; Baker, G. L. *Langmuir* **2008**, *24*, 7663–7673.
- (10) Saren, Q.; Qiu, C. Q.; Tang, C. Y. *Environ. Sci. Technol.* **2011**, *45*, S201–S208.
- (11) Li, X.; De Feyter, S.; Chen, D.; Aldea, S.; Vandezande, P.; Du Prez, F.; Vankelecom, I. F. *Chem. Mater.* **2008**, *20*, 3876–3883.
- (12) Dai, J.; Balachandra, A. M.; Lee, J. I.; Bruening, M. L. *Macromolecules* **2002**, *35*, 3164–3170.
- (13) Deen, W. *AIChE J.* **1987**, *33*, 1409–1425.
- (14) Freger, V. *Langmuir* **2003**, *19*, 4791–4797.
- (15) Wang, X. L.; Tsuru, T.; Nakao, S.; Kimura, S. *J. Membr. Sci.* **1997**, *135*, 19–32.
- (16) Bowen, W. R.; Welfoot, J. S. *Chem. Eng. Sci.* **2002**, *57*, 1121–1137.
- (17) Freger, V. *Environ. Sci. Technol.* **2004**, *38*, 3168–3175.
- (18) Hammond, P. T. *AIChE J.* **2011**, *57*, 2928–2940.
- (19) Yang, Q.; Adrus, N.; Tomicki, F.; Ulbricht, M. *J. Mater. Chem.* **2011**, *21*, 2783–2811.
- (20) Eshet, I.; Freger, V.; Kasher, R.; Herzberg, M.; Lei, J.; Ulbricht, M. *Biomacromolecules* **2011**, *12*, 1169–1177.
- (21) Jiang, W.; Childs, R. F.; Mika, A. M.; Dickson, J. M. *Desalination* **2003**, *159*, 253–266.
- (22) Susanto, H.; Ulbricht, M. *Langmuir* **2007**, *23*, 7818–7830.
- (23) Peeva, P. D.; Pieper, T.; Ulbricht, M. *J. Membr. Sci.* **2010**, *362*, 560–568.
- (24) He, D.; Susanto, H.; Ulbricht, M. *Prog. Polym. Sci.* **2009**, *34*, 62–98.
- (25) Peeva, P. D.; Knoche, T.; Pieper, T.; Ulbricht, M. *Sep. Purif. Technol.* **2012**, *92*, 83–92.
- (26) Pieracci, J.; Crivello, J. V.; Belfort, G. *Chem. Mater.* **2002**, *14*, 256–265.
- (27) Peeva, P. D.; Million, N.; Ulbricht, M. *J. Membr. Sci.* **2012**, *390–391*, 99–112.
- (28) Zundel, G. *J. Membr. Sci.* **1982**, *11*, 249–274.
- (29) Behar, D.; Fessenden, R. W.; Hornak, J. P. *Radiat. Phys. Chem.* **1982**, *20*, 267–273.
- (30) Shkolnik, S.; Behar, D. *J. Appl. Polym. Sci.* **1982**, *27*, 2189–2196.
- (31) Kim, S. J.; Park, S. J.; Kim, S. I. *Smart Mater. Struct.* **2004**, *13*, 317–322.
- (32) Yamaguchi, T.; Ibe, M.; Nair, B. N.; Nakao, S. *J. Electrochem. Soc.* **2002**, *149*, A1448–A1453.
- (33) Bingöl, B.; Meyer, W. H.; Wagner, M.; Wegner, G. *Macromol. Rapid Commun.* **2006**, *27*, 1719–1724.
- (34) Ellis, J.; Anstice, M.; Wilson, A. D. *Clin. Mater.* **1991**, *7*, 341–346.
- (35) Wu, Y. H.; Liu, Y. L.; Chang, Y.; Higuchi, A.; Freeman, B. D. *J. Membr. Sci.* **2010**, *348*, 47–55.
- (36) Andrzejewska, E. *Prog. Polym. Sci.* **2001**, *26*, 605–665.
- (37) Kurdkar, D. L.; Peppas, N. A. *Macromolecules* **1994**, *27*, 4084–4092.
- (38) He, H.; Li, L.; Lee, L. J. *React Funct Polym* **2008**, *68*, 103–113.
- (39) Zhang, S.; Xu, T.; Wu, C. *J. Membr. Sci.* **2006**, *269*, 142–151.
- (40) Mika, A.; Childs, R.; Dickson, J.; McCarry, B.; Gagnon, D. *J. Membr. Sci.* **1997**, *135*, 81–92.
- (41) Bernstein, R.; Belfer, S.; Freger, V. *Langmuir* **2010**, *26*, 12358–12365.
- (42) Dalwani, M.; Bargeman, G.; Hosseiny, S.; Boerrigter, M.; Wessling, M.; Benes, N. E. *J. Membr. Sci.* **2011**, *381*, 81–89.
- (43) Kang, G.; Liu, M.; Lin, B.; Cao, Y.; Yuan, Q. *Polymer* **2007**, *48*, 1165–1170.
- (44) Boussu, K.; Zhang, Y.; Cocquyt, J.; Van Der Meer, P.; Volodin, A.; Van Haesendonck, C.; Martens, J.; Van der Bruggen, B. *J. Membr. Sci.* **2006**, *278*, 418–427.
- (45) Van der Bruggen, B.; Mänttäri, M.; Nyström, M. *Sep. Purif. Technol.* **2008**, *63*, 251–263.
- (46) Manttari, M.; Pihlajamaki, A.; Nystrom, M. *J. Membr. Sci.* **2006**, *280*, 311–320.

(47) Schaep, J.; Van der Bruggen, B.; Vandecasteele, C.; Wilms, D. *Sep. Purif. Technol.* **1998**, *14*, 155–162.

(48) Liu, X.; Bruening, M. L. *Chem. Mater.* **2004**, *16*, 351–357.

(49) Nilsson, M.; Trägårdh, G.; Östergren, K. *J. Membr. Sci.* **2008**, *312*, 97–106.

(50) Malaisamy, R.; Bruening, M. L. *Langmuir* **2005**, *21*, 10587–10592.

(51) Bason, S.; Kedem, O.; Freger, V. *J. Membr. Sci.* **2009**, *326*, 197–204.

(52) Stanton, B. W.; Harris, J. J.; Miller, M. D.; Bruening, M. L. *Langmuir* **2003**, *19*, 7038–7042.

(53) Szymczyk, A.; Fievet, P. *J. Membr. Sci.* **2005**, *252*, 77–88.

(54) Tieke, B.; Van Ackern, F.; Krasemann, L.; Toutianoush, A. *Eur. Phys. J. E* **2001**, *5*, 29–39.

(55) Jin, W.; Toutianoush, A.; Tieke, B. *Langmuir* **2003**, *19*, 2550–2553.

(56) Schaep, J.; Vandecasteele, C.; Wahab Mohammad, A.; Richard Bowen, W. *Sep. Purif. Technol.* **2001**, *22*, 169–179.

(57) Van Gestel, T.; Vandecasteele, C.; Buekenhoudt, A.; Dotremont, C.; Luyten, J.; Leysen, R.; Van der Bruggen, B.; Maes, G. *J. Membr. Sci.* **2002**, *209*, 379–389.

(58) Nanda, D.; Tung, K. L.; Li, Y. L.; Lin, N. J.; Chuang, C. J. *J. Membr. Sci.* **2010**, *349*, 411–420.